Redox-responsive 1D-assembly built from cucurbit[8]uril and a water-soluble metalloporphyrin-based tecton

Shagor Chowdhury, Paul Hennequin, Olivier Cala, Sandrine Denis-Quanquin, Éric Saint-Aman, Denis Frath, Floris Chevallier, Christophe Bucher

Redox-responsive 1D-assembly built from cucurbit[8]uril and a water-soluble metalloporphyrin-based tecton

Shagor Chowdhury[a], Paul Hennequin[a], Olivier Cala[b], Sandrine Denis-Quanquin[a], Éric Saint-Aman[c], Denis Frath[a], Floris Chevallier[a*] and Christophe Bucher[a*]

[a]*Univ Lyon, ENS de Lyon, CNRS UMR 5182, Laboratoire de Chimie, 69342 Lyon, France*

[b]*Univ Lyon, ENS de Lyon, UCBL, CNRS UMR 5280, Centre de RMN à Très Hauts Champs, 69100 Villeurbanne, France*

[c]*Univ Grenoble Alpes, CNRS UMR 5250, Département de Chimie Moléculaire, 38000 Grenoble, France*

Received date (to be automatically inserted after your manuscript is submitted)

Accepted date (to be automatically inserted after your manuscript is accepted)

Dedicated to Pr. Jonathan L. Sessler on the occasion of his 70th birthday

ABSTRACT: A linear orphyrin-based tecton bearing two 4,4'bipyridinium units (viologens) and two monomethyl-ether triethylene glycol-substituted phenyl substituants at the *meso* positions was synthesized and characterized. The latter was involved in the redox-triggered formation of linear supramolecular assemblies with cucurbit[8]uril (CB[8]) cavitands in aqueous media. The CB[8]-promoted intermolecular π-dimerization of the viologen cation radicals introduced at the meso positions of the porphyrin platform has been brought to light through the diagnostic signatures of the 1:2 host-guest ternary caviplexes formed between viologen and CB[8] and by spectroscopic data collected after electrochemical reduction of the viologen-based tectons.

KEYWORDS: π-dimer, self-assembly, viologen, cucurbituril, porphyrin

INTRODUCTION

Molecular self-assembly has been shown to play a major role in the emergence and development of life on Earth.[1,2] It is now widely used to provide easy access to complex architectures and supramolecular materials or to organize molecules in electronic devices.[3] These fascinating properties have led chemists to focus on the development of supramolecular systems capable of performing specific tasks and functions in controlled manners. A wide range of stimuli have already been considered to operate responsive-molecular systems including heat, pH, electric fields, magnetic fields, mechanical forces, sound, light, microwaves and chemical reactions. Compared to other stimuli, the use of electrons is particularly attractive as it can simultaneously induce changes in the charge and/or in the spin states of molecules while being fully compatible with the operation constraints of electronic devices. Another advantage is that the oxidation or reduction of responsive molecular elements can potentially be achieved either electrochemically, photochemically or by addition of suitable chemical oxidants/reductants. Different strategies have been pursued so far taking advantage of electron transfers

* Correspondence to: christophe.bucher@ens-lyon.fr (Christophe Bucher), floris.chevallier@ens-lyon.fr (Floris Chevallier).

centred either on metallic or organic building/responsive elements. The ability of of π-conjugated organic radicals to self-assemble into π-dimers has proven to be of particular interest for the development of electron responsive molecular switches and machinery parts.[4] The formation of intermolecular π-dimers have yet been successfully employed for the construction of zero-,[5] one-,[6] two-,[7] and three-[8] dimensional supramolecular architectures. In line with these ideas, our recent efforts have aimed at achieving an electrochemical control over the formation of supramolecular assemblies by exploiting the high affinity of CB[8] cavitands for viologen based π-dimers; the underlying idea being that the dimensionality of the assemblies (1D or 2D) could be tuned with the number and relative orientation of the viologen units introduced on a given organic scaffold. The studies detailed below involve monomers incorporating a porphyrin ring as a structuring element, as readout molecular tools and as a functional unit that could provide the resulting supramolecular materials with unique sensing, catalytic or photochemical properties. This study is a continuation of previous works carried out on photo- and redox-responsive 2D-supramolecular assembly involving cucurbit[8]uril and viologen-based tectons.[7] In the current study, we report the CB[8]-mediated intermolecular π-dimerization of the porphyrin-viologen linear tectons $\mathbf{7}^{4+}$ yielding a 1D assembly (Figure 1).

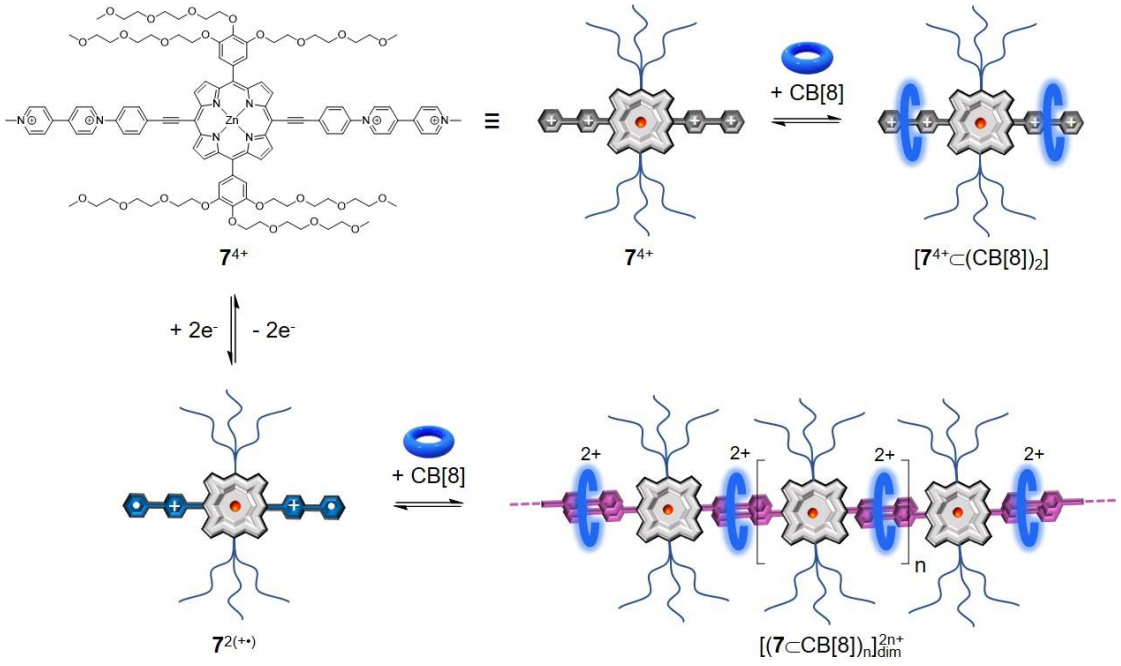

Figure 1. Schematic representation of the targeted electron-responsive 1D-self-assembly process.

RESULTS AND DISCUSSION

Synthesis

The multi-step synthesis of the targeted viologen-porphyrin conjugate $\mathbf{7}^{4+}$ is summarized in Scheme 1. The intermediate **3** was obtained using a previously reported procedure.[9] The starting point is an S_N2 alkylation of 3,4,5-trihydroxybenzaldehyde with triethylene glycol methyl ether tosylate (MTEG-Tos) affording the corresponding MTEG-substituted benzaldehyde **1** in 50% yield. The ABAB *meso*-free porphyrin **2** was then synthesized in 50% yield as a product of a Brønsted acid-catalyzed condensation of 2,2′-dipyrrolylmethane with the MTEG-substituted benzaldehyde **1**, followed by oxidation with DDQ of the porphyrinogen intermediate. Subsequent regioselective α-bromination of the two remaining

meso-free positions with *N*-bromosuccinimide afforded **3** in 98% yield. The key amine-substituted intermediate **4** was then obtained in 90% yield as the main product of a palladium-catalyzed Sonogashira cross-coupling reaction between **3** and 4-ethynylaniline. The aniline-substituted porphyrin derivative **4** was subsequently subjected to a double Zincke coupling reaction involving the activated viologen-based precursor $\mathbf{5}^{2+}$ as a co-reactant to afford the free base porphyrin-viologen $\mathbf{6}^{4+}$ in 58% yield. The targeted compound $\mathbf{7}^{4+}$ was ultimately obtained in a nearly quantitative yield by metalation of the porphyrin macrocycle with an excess of zinc(II) acetate. The free base and metallated species were both isolated under the form of chloride or hexafuorophosphate salts using standard anion metathesis protocols.

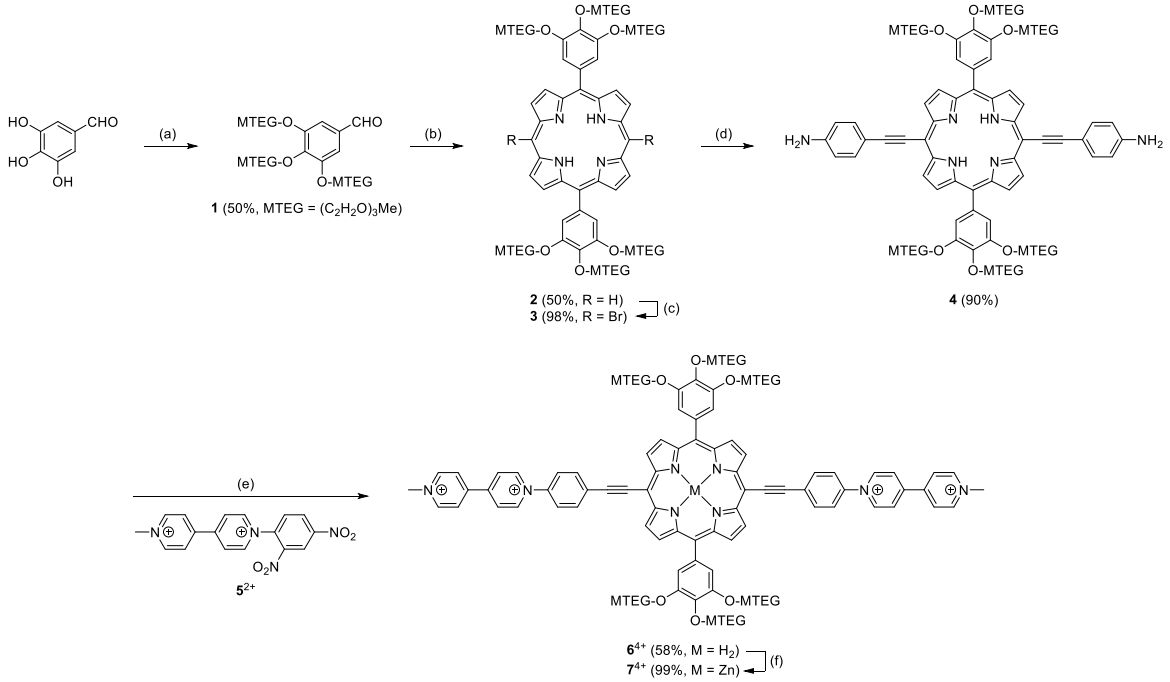

Scheme 1. Synthesis of the ditopic tecton $\mathbf{7}^{4+}$. (a) MTEG-OTs, K_2CO_3, DMF, 100 °C, 72 h. (b) 2,2′-dipyrrolylmethane, TFA, $CHCl_3$, 25 °C, 14 h; then DDQ, 25 °C, 3 h. (c) NBS, $CHCl_3$, -40 °C, 60 min. (d) 4-ethynylaniline, $Pd_2(dba)_3$, $AsPh_3$, Et_3N, THF, 50 °C, 24 h. (e) $\mathbf{5}^{2+}$, EtOH, CH_3CN, 70 °C, 18 h. (f) $Zn(OAc)_2$, CH_3CN, 25 °C, 16 h.

NMR characterizations

The proton NMR spectra of $\mathbf{6}(PF_6)_4$ and $\mathbf{7}(PF_6)_4$ recorded in deuterated dimethyl sulfoxide are shown in Figure 2. The accurate attribution of the aromatic signals was achieved from careful analyses of the ^{1}H-NMR spectrum and of the associated COSY and ROESY maps. The most deshielded signal in the spectrum of the freebase $\mathbf{6}(PF_6)_4$ and of the metallated porphyrin $\mathbf{7}(PF_6)_4$ is attributed to the *β*-hydrogen atoms Hh which are influenced by the ring current of the porphyrin and by the electron-withdrawing character of neighboring viologen units. The presence of zinc in the porphyrin cavity induces small upfield shifts of the aromatic protons, more specifically of protons Hh and Hi located at the *β* position of the heterocyclic macrocycle, and of those located on the MTEG-substituents. These shifts are consistent with the known electron-donating effect of the zinc atom on the porphyrin-based π-system.[7] As expected, the presence of the zinc metal within the cavity of the porphyrin ring was also confirmed by the absence of signal below 0 ppm.

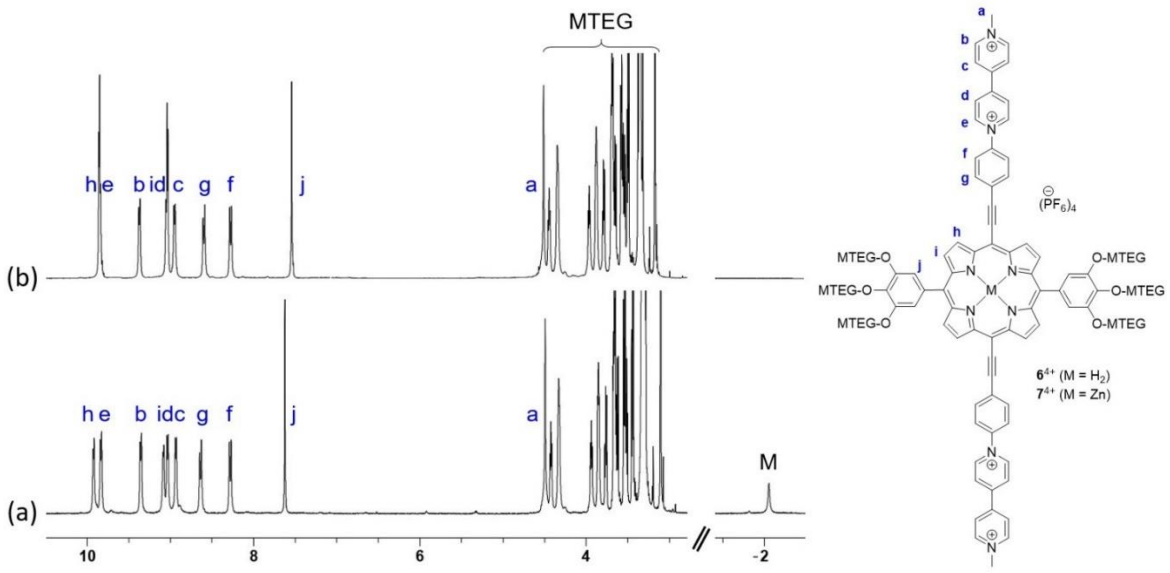

Figure 2. Partial ^{1}H-NMR spectra (400 MHz, DMSO-d_6, 1.0 mM, 298 K) of (a) **6**$(PF_6)_4$ and (b) **7**$(PF_6)_4$.

The chloride salt **7**Cl_4 was also characterized by ^{1}H-NMR spectroscopy in D_2O and DMSO-d_6 (Figure 3c-e). Quite unexpectedly, we found the spectrum recorded in deuterated water (Figure 3e) to display up to nineteen signals in the aromatic region, which turned out to be about twice the number of signals observed in DMSO-d_6 (Figure 3d). These signals were also found to resonate over a much wider window in water (5-11.5 ppm) than in DMSO (7.5-10 ppm). The major role of the solvent and the minor role of the anions on the NMR signature of $\mathbf{7}^{4+}$ were eventually confirmed upon showing that the spectra of **7**$(PF_6)_4$ and of **7**Cl_4 are identical in DMSO-d_6 (Figure 3c-d). The signals attributed to the viologen moieties could only be identified from careful analyses of the ^{1}H-NMR data (coupling constant of about 5-6 Hz) and of the COSY/ROESY/HSQC maps (see the supplementary material). Similar differences were observed between NMR data collected for the free base **6**Cl_4 in DMSO (Figure 3a) or in water (Figure 3b). The main conclusion drawn from the number of signals monitored in water, and from their relative intensities, is that $\mathbf{7}^{4+}$ and $\mathbf{6}^{4+}$ aggregate in water to yield poorly symmetric self-assembled architectures.

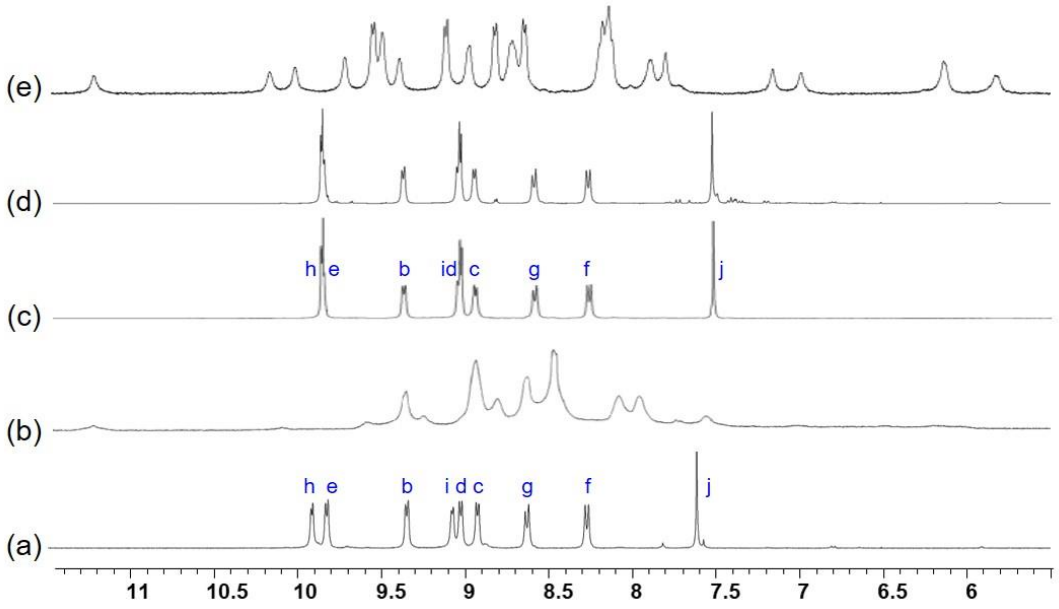

Figure 3. Partial ^{1}H-NMR spectra (400 MHz, 1.0 mM, 298 K) of (a) **6**$(PF_6)_4$ in DMSO-d_6, (b) **6**Cl_4 in D_2O, (c) **7**$(PF_6)_4$ in DMSO-d_6, (d) **7**Cl_4 in DMSO-d_6, and (e) **7**Cl_4 in D_2O.

Several hypotheses can be put forward to account for the complex spectrum recorded in water. The most likely one involves the self-assembly of the porphyrin conjugates $\mathbf{6}^{4+}$ or $\mathbf{7}^{4+}$ leading to the formation of J- or H-aggregates.[10,11] Such aggregation could either lead to a large scale self-assembly of monomers yielding polymers or to the formation of discrete assemblies including a finite number of monomers. As a matter of fact, charged porphyrins have a well-known tendency to form dimers,[12,13] and large-scale aggregates in water.[14-16] Their formation has been shown to depend on the charge, structure and substitution of the porphyrin ring and also on the ionic strength, temperature and pH of the investigation medium. Aggregation is usually revealed by simple NMR measurements, but identification of the aggregation mode usually requires more extensive analyzes of UV-vis absorption spectroscopic data. Our studies have focused on the metallated species **7**Cl_4, showing an NMR signature in water consistent with the formation of a well-defined assembly. The ability of **7**Cl_4 to self-assemble in water was further revealed by studying the influence of concentration. The spectra collected for concentration ranging from 10^{-4} to 10^{-3} M are shown in Figure 4a. These data reveal that dilution leads to a concomitant decrease in the number of signals and in the resonance window. The spectrum recorded at 10^{-3} M remains quite ill-defined but the NMR window has narrowed significantly to reach a value close to that observed with the monomer in organic medium (7 to 10 ppm for the aromatic protons). We also checked the influence of temperature on the aggregation process upon recording the ^{1}H-NMR spectrum of a 10^{-3} M aqueous solution of **7**Cl_4 at different temperature. This study revealed that increasing the temperature of the sample from 298 K to 348 K induces a significant simplification of the spectrum (Figure 4ba), the most relevant ones being a large drop in the number of signals and a narrowing of the chemical shift window. As a conclusion, both the concentration and temperature-dependent experimental data discussed above support the conclusion that the self-assembled species formed in aqueous media get dissociated upon increasing temperature or at concentrations below 10^{-4} M.

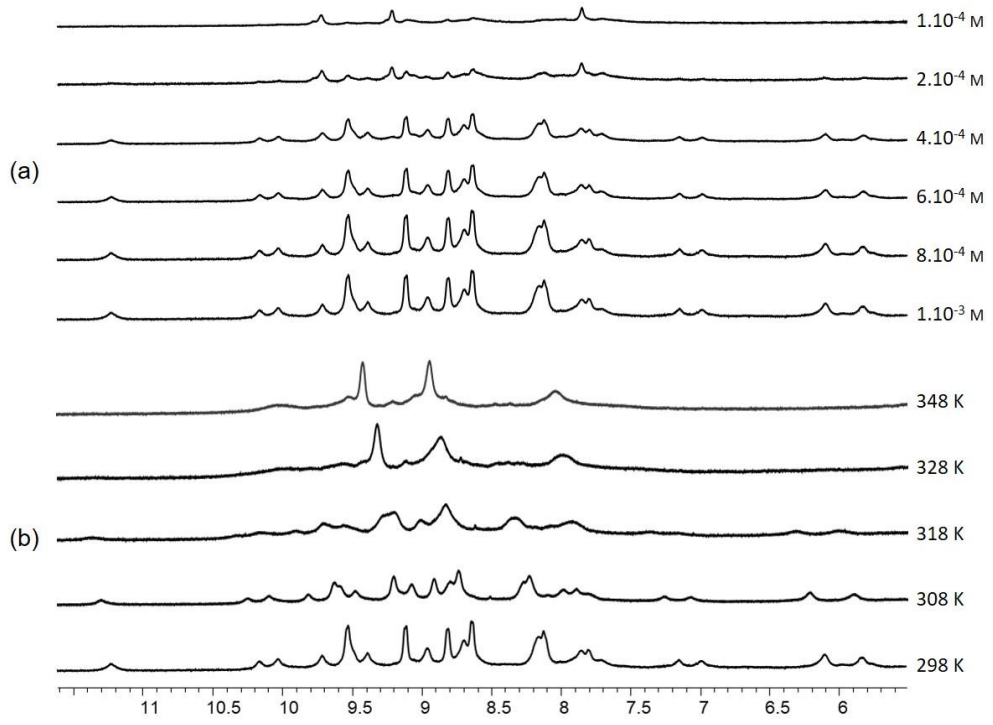

Figure 4. Partial ^{1}H-NMR spectra (D_2O, 400 MHz) of **7**Cl_4 recorded (a) at different concentrations, and (b) at different temperatures.

Further insights into the impact of the solvent on the self-association of $\mathbf{7}^{4+}$ have been provided by diffusion ordered spectroscopy (DOSY) measurements giving access to the diffusion coefficient characteristic of the molecular species present in solution (see the supplementary material). All the data collected in DMSO and in water are consistent with the formation of a monomer in organic medium, and several self-assembled structures in aqueous medium.

The interactions between CB[7] or CB[8] and $\mathbf{7}^{4+}$ in water have also been studied by ^{1}H-NMR measurements. The progressive addition of CB[7] (from 0 to 2 equiv.) to a solution of $\mathbf{7}^{4+}$ in phosphate buffer resulted in the shift of a limited number of signals (Figure 5). These results led to the conclusion that a pseudo-rotaxane product is formed in solution and that the threading of two CB[7] rings per porphyrins does not change the overall symmetry of the assembly, as revealed by the same number of signals observed in the absence and in the presence of CB[7].

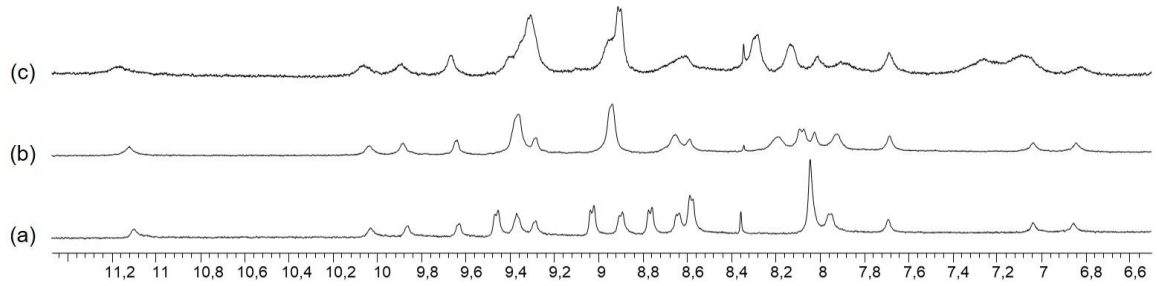

Figure 5. Partial ^{1}H-NMR spectra of $\mathbf{7}Cl_4$ (5.10^{-4} M, 0.1 M phosphate buffer / D_2O, 400 MHz) recorded after addition of (a) 0, (b) 1.0, and (c) 2.0 equivalents of CB[7].

Similar analyses have been conducted in the presence of CB[8] (see the supplementary material). These evolutions reveal that the aggregates of $\mathbf{7}^{4+}$ are dissociated in the presence of CB[8] and that the resulting inclusion complex remains poorly symmetric. Careful analyses of the ^{1}H-NMR, COSY and ROESY correlation maps led us to conclude that the [1:1] inclusion complex [$\mathbf{7}^{4+}\subset$CB[8]] is the only product formed in solution in the presence of CB[8]. It should however be mentioned that [$\mathbf{7}^{4+}\subset$CB[8]] and [$\mathbf{7}^{4+}\subset$(CB[8])$_2$] have been observed on the MS spectra (ESI) of $\mathbf{7}(PF_6)_4$ recorded in the presence of CB[8] (see the supplementary material).

UV-visible absorption measurements

Further insights into the aggregation mode of $\mathbf{7}Cl_4$ in water have been provided by UV-vis absorption measurements. The UV-vis absorption spectrum collected for an acetonitrile solution of $\mathbf{7}(PF_6)_4$ at 10^{-3} M exhibits one Soret band centered at λ_{max} = 446 nm (208000 $M^{-1}.cm^{-1}$) and a much less intense Q band at λ_{max} = 663 nm (54000 $M^{-1}.cm^{-1}$). The absence of aggregation in these conditions was brought to light by the linear evolution of the intensity measured at λ_{max} = 446 nm as a function of concentration in the 10^{-3} to 10^{-6} M range. This conclusion was also further supported by the curves shown in Figure 6a revealing that the shape and max wavelengths of the porphyrin-based signals do not change with concentration. Similar measurements carried out in water revealed that the UV-Visible absorption spectrum of $\mathbf{7}Cl_4$ (10^{-4} to 10^{-5} M) exhibits also two absorption bands, at λ_{max} = 456 nm (194000 $M^{-1}.cm^{-1}$ calculated at 1 mM) and at λ_{max} = 674 nm (63000 $M^{-1}.cm^{-1}$ calculated at 1 mM). The curves collected in Figure 6b then show that increasing the concentration of $\mathbf{7}Cl_4$ from 10^{-5} to 10^{-3} M leads to a bathochromic shift of both the Soret (456 to 460 nm) and Q-bands (674 to 679 nm). The effect of concentration on the spectroscopic signature of $\mathbf{7}^{4+}$ in water was then further revealed by the non-linear evolution of the absorption intensities collected in the 10^{-3} to 10^{-6} M range. Overall, these concentration-dependent data are thus consistent with the conclusion that $\mathbf{7}Cl_4$ aggregates in water. This conclusion is also supported by the known propensity of cationic

porphyrins to self-assemble in water producing either extended J- or H-aggregates.[10,11] One first conclusion that can be drawn from these literature data and from the limited magnitude of the modifications observed over the 10^{-3} to 10^{-6} M concentration range is that the porphyrin rings remain fairly distant from each other in the aggregated form.

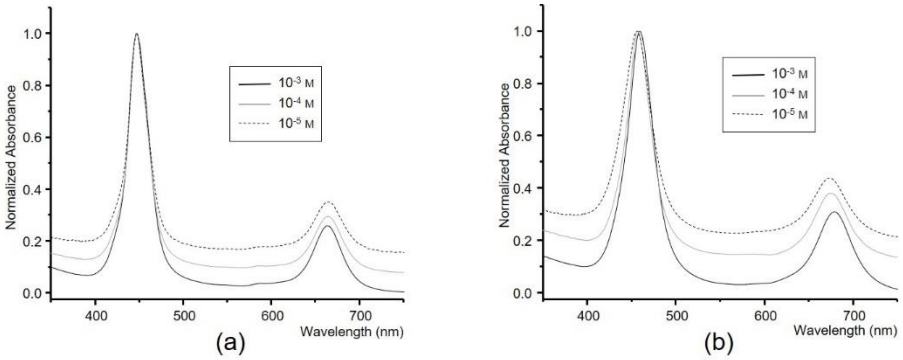

Figure 6. Normalized UV-visible absorption spectra recorded at different concentrations of (a) **7**$(PF_6)_4$ in CH_3CN, and (b) **7**Cl_4 in H_2O.

Similar investigations have been carried out with the free base **6**Cl_4. As can be seen in Figure 7, the UV-visible absorption spectrum recorded in water from 10^{-3} to 10^{-6} M display three absorption bands centered at λ_{max} = 429 nm (21000 $M^{-1}.cm^{-1}$), 617 nm (40000 $M^{-1}.cm^{-1}$) and 701 nm (20000 $M^{-1}.cm^{-1}$). The concentration-induced self-aggregation of the free base was in this case readily revealed by a significant deviation from the Beer-Lambert law (Figure 7b) and by the apparition of a new absorption band developing at λ_{max} = 452 nm (70000 $M^{-1}.cm^{-1}$, C = 10^{-3} M).

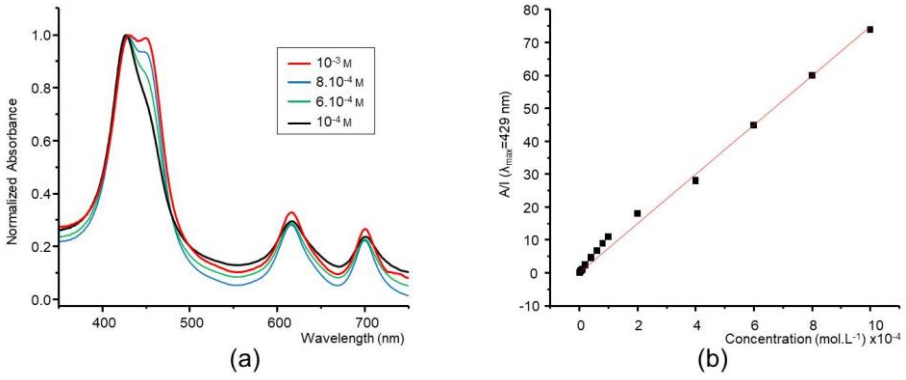

Figure 7. (a) Normalized UV-visible absorption spectra recorded at different concentrations of **6**Cl_4 in H_2O, and (b) variation of the absorbance measured at λ = 429 nm for **6**Cl_4 in H_2O as function of concentration

Increasing the ionic strength of the aqueous medium was found to have an effect similar to concentration. As can be seen in Figure 8a, the progressive addition of KNO_3 (up to 1.0 M) to an aqueous solution of **7**Cl_4 (10^{-5} M) led to a red shift of the Soret (456 to 464 nm) and Q bands (673 to 683 nm) coming along with a loss of half of their intensities. It needs to be mentioned that a similar behavior was observed upon addition of dimethylviologen (up to 0.1 M) leading to a large decrease in intensity and red shift of the Soret (+4 nm) and Q bands (+13 nm) (see the supplementary material). As observed upon varying the concentration in monomer, addition of KNO_3 to an aqueous solution of the free base **6**Cl_4 (10^{-5} M) led to the emergence of a second band centered at 450 nm and to a weak red shift of both Q bands ($4 \geq \Delta\lambda \geq 2$ nm) (Figure 8b).

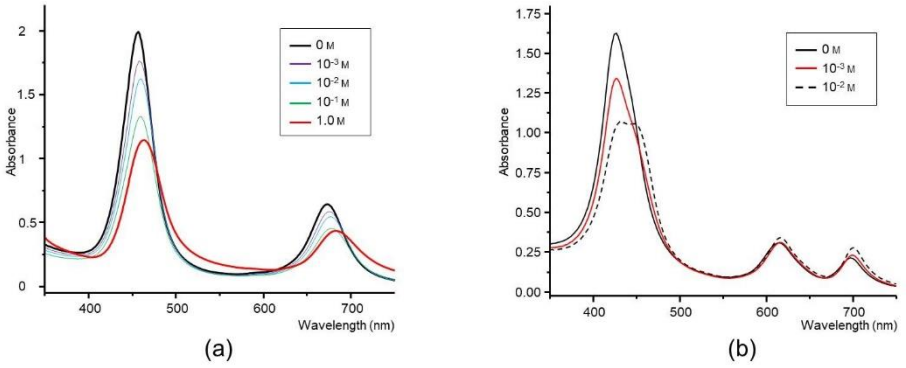

Figure 8. UV-Visible absorption spectra recorded for in H_2O at different concentration of KNO_3 for (a) **7**Cl_4 (10^{-5} M) and (b) **6**Cl_4 (10^{-5} M).

All these data recorded at different concentrations or at different ionic strengths are thus consistent with the aggregation of **6**Cl_4 and **7**Cl_4 in water to afford very different assemblies. As a general statement, a red-shift of the Soret band is usually indicative of a slipped parallel (J-aggregate) arrangement of the porphyrin units while a blue shift is indicative of face to face (head-to-head, H-aggregates) arrangements. The red shift of the Soret band observed upon increasing the concentration in **7**Cl_4 and **6**Cl_4 or the ionic strength of the medium are therefore rather supporting the formation of J-aggregates. The much larger changes observed with the free base **6**Cl_4 than with the zinc complex **7**Cl_4 also indicate that their aggregation modes are different and that the porphyrin chromophores are likely to be closer in $(\mathbf{6}^{4+})_n$ than in $(\mathbf{7}^{4+})_n$.

Electrochemical characterizations in organic medium

The electrochemical signatures of the free base and metalated compounds **6**$(PF_6)_4$ and **7**$(PF_6)_4$ have first been investigated in DMF using tetra-*n*-butylammonium perchlorate (TBAP) as an electrolyte. Both compounds display similar signatures featuring four consecutive reduction waves and one oxidation wave in the accessible potential window (Table 1).

Table 1. Potential values measured by cyclic voltammetry for **6**$(PF_6)_4$ and **7**$(PF_6)_4$ in DMF and in H_2O.

	Solvent	E^{4c} (n, ΔE_p) **$P^{\bullet-}/P^{2-}$**	E^{3c} (n, ΔE_p) **$P/P^{\bullet-}$**	E^{2c} (n, ΔE_p) **$V^{+\bullet}/V^0$**	E^{1c} (n, ΔE_p) **$V^{2+}/V^{+\bullet}$**	E^{1a} (n, ΔE_p) **$P^+/P^{+\bullet}$**
MeVMe$(PF_6)_2$	DMF	n/a	n/a	-1.163[b] (1, 62)	-0.774[b] (1, 60)	n/a
6$(PF_6)_4$	DMF	-1.816[c]	-1.304[b] (1, 64)	-1.051[b] (2, 62)	-0.743[b] (2, 55)	0.686[a]
7$(PF_6)_4$	DMF	-2.065[c]	-1.547[b] (1, 66)	-1.076[b] (2, 64)	-0.763[b] (2, 63)	0.484[a]
MeVMe$(Cl)_2$	H_2O	n/a	n/a	-0.99[b] (1, 77)[b]	-0,654[b] (1, 60)	n/a
7$(Cl)_4$	H_2O	n/a	n/a	-0.645[b] (2, 157)	-0.402[b] (2, 119)	n/a

Measured by CV, 2.10^{-4} M in DMF/TBAP (0.1 M, E(V) *vs.* Fc^+/Fc), or in an aqueous phosphate buffer (0.1 M, pH = 7, E(V) *vs.* AgCl/Ag (KCl sat) at a vitreous carbon working electrode Ø = 3 mm, 298 K, $\nu = 0.1$ V·s^{-1}. [a] Anodic peak potential. [b] Half wave potential. [c] Cathodic peak potential.

In the case of $\mathbf{7}^{4+}$, the first reversible reduction wave centered at $(E_{½})^{1c} = -0.763$ V is attributed to the one-electron reduction of the two viologens units (one electron per viologen) yielding the dicationic compound $\mathbf{7}^{2(+\bullet)}$. The Nernstian character ($I_{pa} / I_{pc} \approx 1$, $\Delta E_p \approx 60$ mV, $I_p = \alpha\nu^{½}$, see Figure 9 and Figure 10) of the reduction wave indicates the absence of chemical reactions coupled to the electron transfer in our experimental conditions (1 mM in DMF). The second reversible reduction wave centered at $(E_{½})^{2c} = -1.076$ V is then attributed to the second one-electron reduction of the viologen units

(one electron per viologen) leading to the neutral quinonic species $\mathbf{7}^{0}$. Here again, the ΔE_p value of about 64 mV calculated for the second reduction wave suggests the absence of communication/interactions between the viologen centers. Another evidence supporting this assumption is the rather short stability domain of the cation-radical state in $\mathbf{7}^{2(+\bullet)}$, $\Delta E = (E_{½})^{2c} - (E_{½})^{1c} = 313$ mV, the latter value being similar to the one measured in the same conditions for a reference molecule like dimethyl viologen (Me**V**Me^{2+}) ($\Delta E = 336$ mV). The two remaining reversible reduction waves of low intensities observed at $(E_{½})^{3c} = -1.547$ V and $(E_{½})^{4c} = -2.065$ V have been attributed to the one-electron reductions of the porphyrin skeleton yielding successively the anion radical $\mathbf{7}^{\bullet-}$ and the dianion $\mathbf{7}^{2-}$, respectively. On the anodic side, the weakly intense and poorly reversible wave observed at $E^{1a} = 0.484$ V is attributed to the one electron oxidation of the porphyrin ring.

The free base porphyrin $\mathbf{6}^{4+}$ has been also studied in the same experimental conditions. Selected values recorded with this compound are collected in Table 1. These data reveal that the metal has a significant effect on the porphyrin-centered redox processes with potential shifts ($\Delta E \approx -200$ mV) in agreement with the known stabilizing effect of the zinc atom on the porphyrin-based π system. The values collected in Table 1 also bring to light that the viologen-based reduction potentials are only weakly affected by the presence of the zinc ion in the cavity of the porphyrin ring (see the supplementary material).

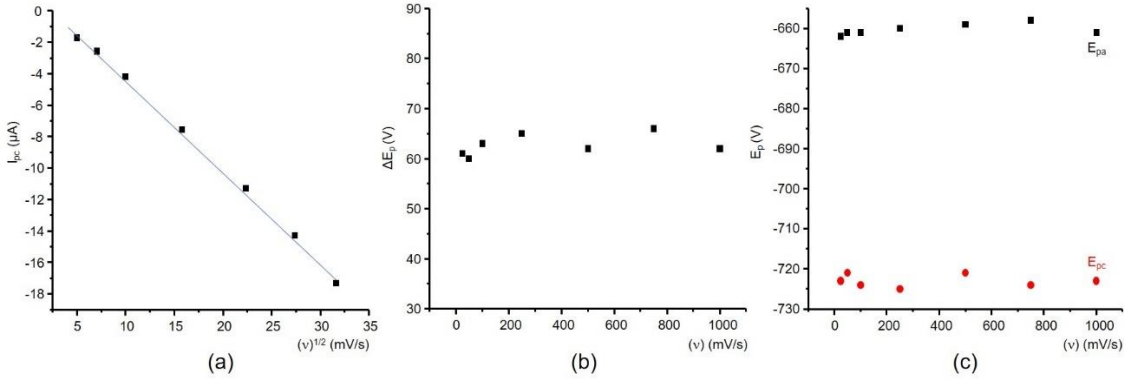

Figure 9. Variations of the (a) peak current, (b) anodic (E_{pa}) and cathodic (E_{pc}) peak potentials values, and (c) peak to peak potential shift (ΔE_p) as a function of scan rate (v in mV/s) (measured for $\mathbf{7}(PF_6)_4$ by CV in DMF (0.1 M TBAP) at a glassy carbon working electrode (Ø = 3 mm, E in V *vs.* Ag^+/Ag 10^{-2} M).

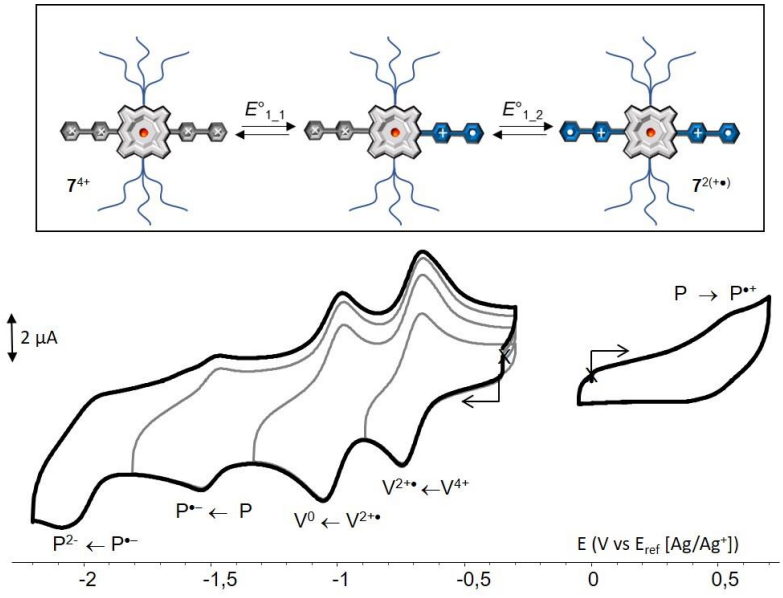

Figure 10. Voltammetric curves of a DMF (TBAP 0.1 M) solution of **7**$(PF_6)_4$ (1.10^{-3} M) recorded at a glassy carbon working electrode (Ø = 3 mm, *E vs.* Ag^+/Ag (10^{-2} M), ν = 0.1 $V.s^{-1}$).

Both the free base $\mathbf{6}^{4+}$ and the zinc complex $\mathbf{7}^{4+}$ have been submitted to spectro-electrochemical characterizations to provide further insights into the fate of the reduced species. These studies have been carried out in a glove box using a conventional three-electrode setting and an all quartz immersion probe. The exhaustive two-electron reduction (one electron per viologen) of **7**$(PF_6)_4$ (1.66 10^{-4} M) in DMF (0.1 M TBAP) solution has been performed in a potentiostatic regime involving setting the potential of the platinum working electrode at – 0.94 V *vs.* $E_{ref}[Ag^+/Ag$ (0.01 M)]. The advancement/completion of the electrolysis was checked by steady-state voltammetry measurements carried out at a rotating disk electrode. As can be seen in Figure 11A, the exhaustive two-electrons reduction of **7**$(PF_6)_4$ led to a slight broadening of the porphyrin-based Soret band coming along with a significant bathochromic shift, of about 6 nm, of its maximum wavelength (from 451 to 457 nm) accompanied with a weak hyperchromic effect. These minor changes indicate that the electron transfer centered on the viologens has a limited impact on the electron density of the porphyrin-based π-system. The novel set of absorption bands developing between 500 and 800 nm, overlapping with the porphyrin-based Q band, is attributed to a series of transitions centered on the electrogenerated viologen cation-radical. Our experiments also revealed that the electrochemical conversion of $\mathbf{7}^{4+}$ into $\mathbf{7}^{2(+\bullet)}$ is fully reversible at the electrolysis time scale (30 min) and that the electrogenerated species $\mathbf{7}^{2(+\bullet)}$ do not form π-dimers in these experimental conditions, as revealed by the absence of diagnostic absorption bands in the near IR region (~900 nm) and by the standard ΔE_p value of about 60 mV measured on the first viologen-based CV wave. Further investigations carried out on the free base $\mathbf{6}^{4+}$ led to similar findings with a spectroscopic signature recorded after bulk electrolysis at E_{app} = -0.94V (*vs.* $E_{ref}[Ag^+/Ag]$) in agreement with the formation of the di-radical species $\mathbf{6}^{2(+\bullet)}$ (Figure 11B).

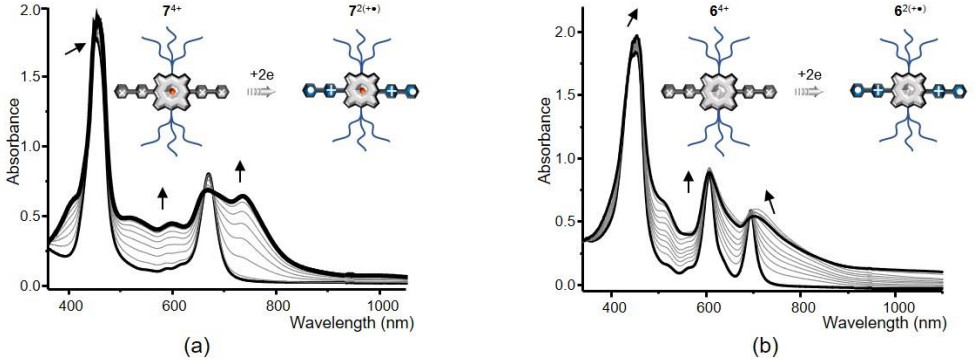

Figure 11. UV-vis spectra recorded during the exhaustive one-electron reduction (per viologen) of (a) **7**$(PF_6)_4$ (1.66 10^{-4} M) and (b) **6**$(PF_6)_4$ (1.11 10^{-4} M) in DMF (0.1 M TBAP) using a platinum plate working electrode whose potential was fixed at E_{app} = -0.94 V *vs.* $E_{Ag^+/Ag}$ (10 mL, l = 1 mm, t ≈ 30 min).

Association with CB[8], electrochemical and spectro-electrochemical studies in aqueous medium

We have studied the ability of CB[8] to promote the intermolecular π-dimerization of the two-electron reduced species $\mathbf{7}^{2(+\bullet)}$ in water to yield the targeted 1D self-assembled polymers (Figure 12). These studies have also been conducted with CB[7], used here as a reference only capable of yielding discrete host-guest caviplexes with $\mathbf{7}^{2(+\bullet)}$.

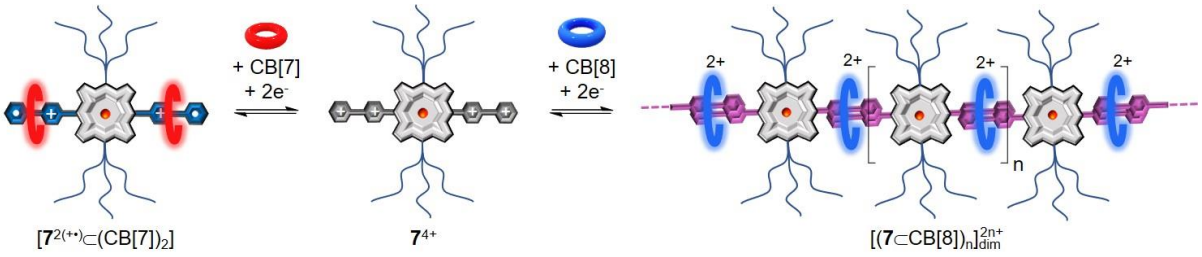

Figure 12. Schematic representation showing the expected binding modes between the two-electron reduced species $\mathbf{7}^{2(+\bullet)}$ and CB[7] or CB[8].

The electrochemical properties of $\mathbf{7}Cl_4$ have been investigated by cyclic voltammetry measurements carried out in a phosphate buffer (pH = 7, 0.1 M) at a vitreous carbon electrode. The CV curve recorded at 2.10^{-4} M displays two consecutive reduction waves at $E^{1c} = -0.402$ and $E^{2c} = -0.645$ V (*E vs.* Ag^+/Ag) attributed to the successive formation of $\mathbf{7}^{2(+\bullet)}$ and $\mathbf{7}^0$, respectively (Table 1). The data depicted in Figure 13 reveal that the main characteristics of the first reduction wave evolve to a great extent with scan rate. The current remains limited by diffusion but the peak potential measured in the forward scan happens to shift quite significantly towards more negative values with increasing scan rates. This irreversibility can be linked to the aggregation of $\mathbf{7}^{4+}$ in aqueous medium.

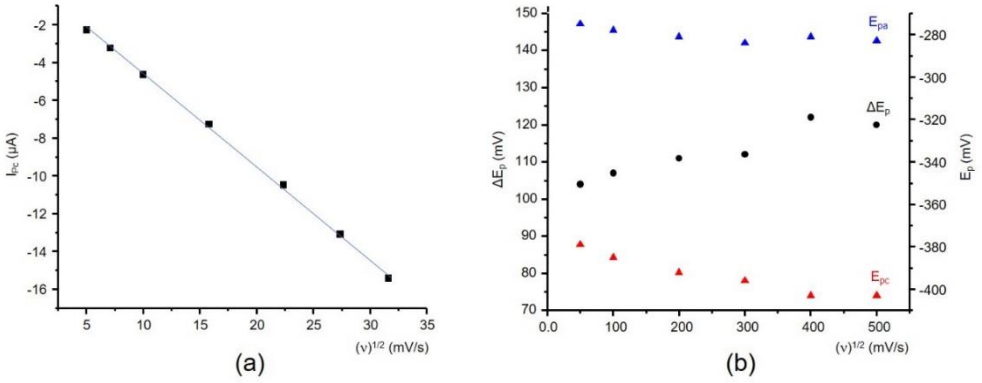

Figure 13. Variations of the (a) peak current, (b) anodic (E_{pa}), cathodic (E_{pc}) peak potentials and peak to peak potential shift (ΔE_p) as a function of scan rate (v in mV/s) (measured for $\mathbf{7}Cl_4$ by CV in a phosphate buffer (0.1 M, pH = 7) at a glassy carbon working electrode (Ø = 3 mm, E in V *vs.* AgCl/Ag).

The relative affinity of CB[8] for $\mathbf{7}^{4+}$ and $\mathbf{7}^{2(+\bullet)}$ was assessed from CV data focusing on the first viologen-centered reduction wave. The data shown on Figure 14a reveal that the addition of CB[8] leads to a progressive decrease in the intensity of the initial wave at $E_p = -0.426$ V in favor of a new wave developing at a less negative potential value ($E_p = -0.345$ V) attributed to the reduction of the inclusion complex formed between $\mathbf{7}^{4+}$ and CB[8]. Both waves are still clearly observed on the CV curve recorded in the presence of 0.5 equivalent of CB[8] (blue line in Figure 14a) while only the second wave developing at $E_p = -0.345$ V remains visible after addition of one molar equivalent of CB[8] (red line in Figure 14a). The peak potential of the second viologen-centered reduction was found to shift to a much greater extent upon addition of CB[8], the wave initially observed at $E_p = -0.724$ V being shifted to -1.07 V in the presence of one molar equivalence of CB[8] (red line in Figure 14b). It is worth mentioning that the upper value of the molar ratio reached towards

the end of the titration, CB[8]:$\mathbf{7}^{4+}$ = 1, not only match the ratio needed to form the ideal 1D arrangement shown in Figure 12, it was also imposed by the solubility limit of CB[8] in our experimental conditions (0.1 M phosphate buffer pH = 7).

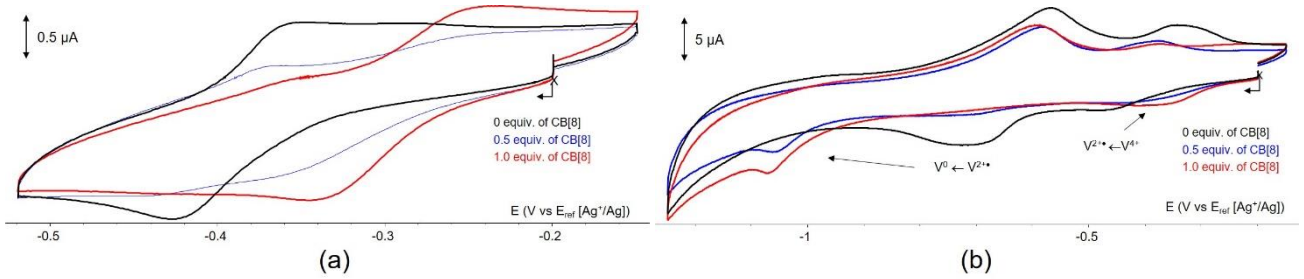

Figure 14. Voltametric curve recorded for **7**Cl$_4$ (5.10^{-4} M) in aqueous phosphate buffer (pH = 7, 0.1 M) in the presence of 0 (red line), 0.5 (blue line) and 1.0 (black line) equivalents of CB[8] (VC Ø = 3 mm, *E vs.* AgCl/Ag) at (a) ν = 25 mV.s^{-1} and (b) ν = 100 mV.s^{-1}

These electrochemical data are thus consistent with the conclusion that the viologen based cation radicals in $\mathbf{7}^{2(+\bullet)}$ are stabilized in the presence of CB[8], the most striking evidence being that the viologen cation radicals are more easily formed and harder to reduce in the presence than in the absence of CB[8]. Based on relevant scientific literature,[7,17,18] this extensive stabilization of the viologen cation radicals in $\mathbf{7}^{2(+\bullet)}$ can be unambiguously attributed to the formation of intramolecular π-dimers included within the cavity of CB[8] hosts, i.e. to the redox triggered transformation of the inclusion complex [$\mathbf{7}^{4+}$⊂CB[8]] into the targeted 1D self-assembled architecture fitting the general formula $([(\mathbf{7}\subset CB[8])_n]^{2n+})_{dim}$ (see Figure 12). This hypothesis has been further confirmed upon carrying out similar investigations with CB[7], used as a control prohibiting the formation of π-dimers.[7,19] Selected CV curves recorded during the progressive addition of CB[7] to a solution of $\mathbf{7}^{4+}$ in water are displayed in Figure 15. In contrast to what was observed with CB[8], the presence of CB[7] was found to induce the simultaneous shift of both viologen-centered reduction waves towards more negative potential values, coming along with a significant drop of the current levels. In agreement with previous report on CB[7]-viologen inclusion complexes, such behavior is here consistent with the idea that CB[7] has a weaker affinity for the viologen cation radicals in $\mathbf{7}^{2(+\bullet)}$ than for the dicationic viologens in $\mathbf{7}^{4+}$.[19] The viologen dication and cation radicals end-up become harder to reduce in the presence of CB[7] while the stability domain of $\mathbf{7}^{2(+\bullet)}$ is not significantly modified.

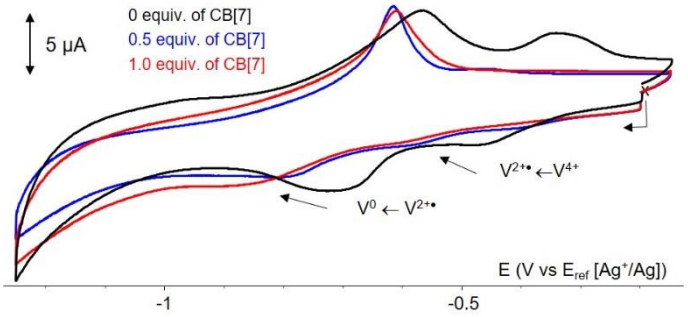

Figure 15. Voltametric curve recorded for **7**Cl$_4$ (5.10^{-4} M) in aqueous phosphate buffer (pH = 7, 0.1 M) in the presence of 0 (red line), 0.5 (blue line) and 1.0 (black line) equivalents of CB[7] (VC Ø = 3 mm, ν = 100 mV.s^{-1}, *E vs.* AgCl/Ag).

The formation of 1D assemblies has been confirmed by UV- vis absorption spectrophotometric measurements conducted in water on the *in situ* generated 2-electron-reduced species $\mathbf{7}^{2(+\bullet)}$ in the absence or in the presence of CBs. The one-electron reduction of both viologen units in $\mathbf{7}^{4+}$ has been carried out in phosphate buffer (pH = 7) using sodium dithionite as a

reductant.[20] Selected UV-vis absorption spectra collected during the progressive addition of $Na_2S_2O_4$ to an aqueous solution of $\mathbf{7}^{4+}$ are shown in Figure 16. These curves reveal that the chemical reduction of $\mathbf{7}^{4+}$ leads to a large drop (about 50%) in the intensity of the Soret band and to a blue shift (27 nm) of the single Q band coming along with a large increase of the baseline signal. Most interestingly, these drastic changes proved to be perfectly reversible, as revealed by the fact that the initial spectrum of $\mathbf{7}^{4+}$ could be fully recovered after gentle bubbling of compressed air through the chemically reduced sample. The curves recovered after addition of $Na_2S_2O_4$ are nevertheless consistent with the existence of chemical steps coupled to the electron transfer. The redox and chemical processes involved in solution upon reduction of $\mathbf{7}^{4+}$ are still poorly understood but the large increase of the base signal, the unusual broadness, splitting and red shift of the initial Soret band strongly suggest the formation of aggregates in solution.[14] Such supramolecular assembly could indeed potentially be formed as a result of the reduction of both viologens (one electron per viologen) in $\mathbf{7}^{4+}$ yielding the far less water soluble species $\mathbf{7}^{2(+\bullet)}$, prone to stacking. The spectroscopic signature recorded in the presence of reducing agent are moreover reminiscent of data reported by different authors with various pyridium-substituted porphyrins where splitting, hypochromicity, broadening and red shifts or blue shifts of Soret bands reveal the formation of mixtures of J- and H-aggregates, respectively.[16,21]

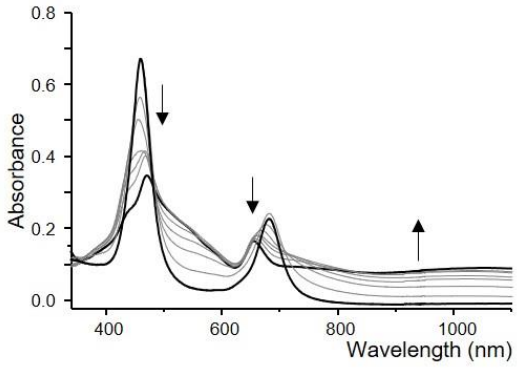

Figure 16. UV-vis spectra of $\mathbf{7}Cl_4$ ($1.1\ 10^{-4}$ M) in phosphate buffer (pH = 7, 0.1 M) recorded over time after addition of $Na_2S_2O_4$ in excess.

Similar studies have been carried out in the presence of CB[8]. Figure 17 shows the UV-vis absorption spectra of $[\mathbf{7}\subset CB[8]]^{4+}$ (formed in situ from a 1:1 mixture of $\mathbf{7}^{4+}$ and CB[8]) after progressive addition of $Na_2S_2O_4$. These curves reveal that the chemical reduction of $[\mathbf{7}\subset CB[8]]^{4+}$ leads to a slight broadening of the porphyrin-based Soret band accompanied with a hypsochromic shift of about 13 nm of its maximum wavelength (from 455 to 442 nm with a clean isosbestic point at 450 nm). These modifications are fully compatible with electron transfers centered on the peripheral viologens having a minor impact on the electron density of the porphyrin-based π-system. This attribution is further supported by the emergence of additional absorption bands between 500 and 800 nm, overlying with the porphyrin-based Q bands, attributed to transitions centered on a viologen cation-radical. Another diagnostic absorption band emerging in the near IR region, at λ_{max} = 960 nm, has been attributed to the formation of viologen-based π-dimers whose energy is proportional to the electronic coupling term arising from frontier-orbital interactions between a pair of equivalent SOMOs.[4] One key conclusion drawn from this analysis is thus that the viologen radicals of the chemically reduced pseudo-rotaxane $[\mathbf{7}\subset CB[8]]^{4+}$ are involved in the formation of self-assembled intermolecular π-dimers. The experimental

data also demonstrate that the proposed supramolecular self-assembly process is fully reversible, as revealed by the fact that a gentle bubbling of compressed air through the sample leads to the regeneration of the initial inclusion complex.

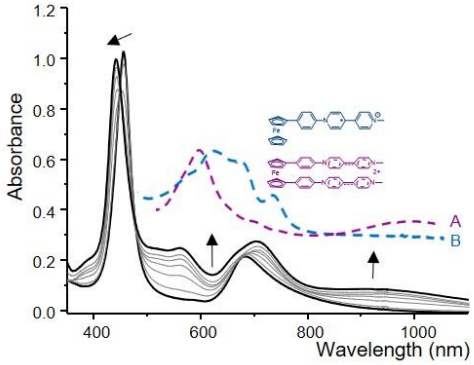

Figure 17. UV-vis spectra of **7**Cl_4 (7 10^{-5} M) and CB[8] (1 equiv.) in phosphate buffer (pH = 7, 0.1 M) recorded over time after addition of $Na_2S_2O_4$ in excess. Reference spectra showing the expected signatures for free radicals and dimers are shown in blue and purple respectively.

Finally, controlled experiments have then be carried out in the presence of CB[7] to confirm the hypotheses raised above. The reduction of $\mathbf{7}^{4+}$ carried out in the presence of two equivalents of CB[7] upon addition of $Na_2S_2O_4$ in excess led to a 15% loss of the initial intensity of the Soret band centered at 455 nm and to the development of a new signals between 500 and 800 nm, overlying with the porphyrin-based Q bands (Figure 18). These results support the conclusion that the electron transfers are centered on the peripheral viologens and that they have minor impact on the electron density of the porphyrin-based π-system. Most importantly, the lack of clear diagnostic absorption bands in the near IR region around 900 nm, demonstrate that the formation of pseudorotaxane with CB[7] inhibits the formation of intermolecular π-dimers.

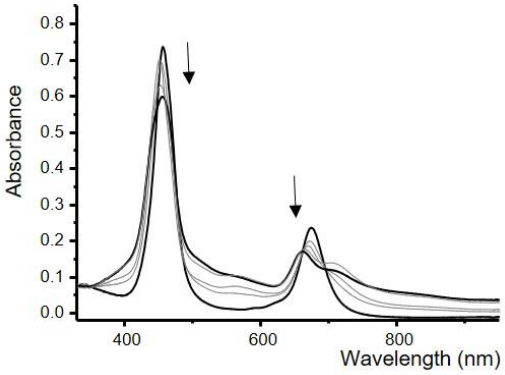

Figure 18. UV-vis spectra of **7**Cl_4 (8.5 10^{-5} M) and CB[8] (2 equiv.) in phosphate buffer (pH = 7, 0.1 M) recorded over time after addition of $Na_2S_2O_4$ in excess.

CONCLUSION

All the experiments carried out with **7**$(PF_6)_4$ and **7**Cl_4 in aqueous and organic media support the conclusions that water promotes self-aggregation of porphyrin $\mathbf{7}^{4+}$. Reduction of $[\mathbf{7}\subset CB[8]]^{4+}$ (one electron per viologen) using sodium dithionite was then found to trigger a CB[8]-mediated intermolecular π-dimerization of the porphyrin-viologen tectons leading to the

formation of a 1D self-assembled species $[(\mathbf{7}\subset CB[8])_n]^{2n+}_{dim}$. Support for these assumptions came from detailed NMR, electrochemical and spectroelectrochemical measurements and from controlled experiments involving CB[7].

EXPERIMENTAL

General

All reagents were obtained commercially unless otherwise noted. All reactions were performed in oven-dried glassware under an argon atmosphere. All solvents were dried and distilled by standard procedures. Flash column chromatography separations were achieved on silica gel (VWR 40-63 μm).

^{1}H-NMR spectra were recorded on Bruker Avance 300, Ascend 400 or Avance III 1GHz spectrometers. Chemical shifts were referenced to residual solvent peaks. Coupling constants values J are given in hertz and chemical shifts δ in ppm. UV/Vis spectra were recorded on an MCS 500 or MCS 601 UV/NIR Zeiss spectrophotometer using all-quartz immersion probes (Hellma Inc.). Mass spectrometry measurements were carried out at the "Centre Commun de Spectrométrie de Masse - Lyon 1" mass spectrometry facility with a MicrOTOFQ II (Bruker) using electrospray ionization (ESI).

Dimethylformamide (Acros Organics™, extra-dry with molecular sieves, water < 0.01%, Acroseal, sealed under argon) was used as purchased for the (spectro)electrochemical studies. The electrolytes tetra-*n*-butylammonium hexafluorophosphate ($TBAPF_6$, Fluka puriss.) and tetra-*n*-butylammonium perchlorate (TBAP) were purchased and used without further purification.

Cyclic voltammetry (CV) and voltammetry with rotating disc electrodes (RDE) were recorded using a SP300 Biologic potentiostat. The analytical studies were conducted inside a glovebox, under a nitrogen atmosphere, in a standard one-compartment, three-electrode electrochemical cell. Tetra-*n*-butylammonium hexafluorophosphate or tetra-*n*-butylammonium perchlorate (TBAP) were used as supporting electrolytes (0.1 M). An automatic ohmic drop compensation procedure was systematically performed when using cyclic voltammetry. Vitreous carbon (Ø = 3 mm) working electrodes (CH Instruments) were polished with 1 mm diamond paste before each recording. Voltamperometry with a rotating disk electrode (RDE) was carried out with a radiometer (CTV101 radiometer analytical) equipment at a rotation rate of 500 rad min^{-1} using a glassy carbon RDE tip (Ø = 3 mm).

Spectroelectrochemical measurements were carried out at room temperature inside a glovebox, under a nitrogen atmosphere, in a standard one-compartment, three-electrode electrochemical cell with a biologic SP300 potentiostat coupled to an MCS 500 or MCS 601 UV/NIR Zeiss spectrophotometer using 1 or 10 mm all-quartz Helmma immersion probes. Electrolyses were conducted at room temperature using platinum plates (10 cm^2) working electrodes and a large piece of carbon felt as a counter-electrode isolated from the electrolytic solution through an ionic bridge. $Ag/AgNO_3$ (CH Instruments, 10^{-2} M + $TBAPF_6$ 10^{-1} M in CH_3CN) was used as a reference electrode.

Synthesis

***3,4,5-Tris-(9-methoxy-1,4,7-trioxanonyl)-benzaldehyde* (1):** To a solution of 3,4,5-trihydroxy-benzaldehyde (154 mg, 1.0 mmol) and tosylated triethylene glycol monomethylether (955 mg, 3.0 mmol) in DMF (10 mL) was added K_2CO_3 (826 mg, 6.0 mmol). The reaction mixture was stirred for 72 h at 100 °C and subsequently poured into aqueous 2 M H_2SO_4 (200 mL). The mixture was extracted with CH_2Cl_2 (3 × 100 mL) and the combined organic layers were dried over $MgSO_4$,

filtered and concentrated under reduced pressure. Purification by flash chromatography on silica gel (EtOAc/heptane: 1/1) gave **1** (296 mg, 50%) as a yellow liquid. ^{1}H NMR (300 MHz, $CDCl_3$) δ (ppm): 3.36 (s, 9H), 3.51-3.88 (m, 30H), 4.19-4.26 (m, 6H), 7.13 (s, 2H), 9.81 (s, 1H). These values are consistent with those reported in the literature.[22]

***5,15-Bis[3,4,5-tris(9-methoxy-1,4,7-trioxanonyl)phenyl]porphyrin* (2):** To a degassed solution of **1** (593 mg, 1.0 mmol) and 2,2′-dipyrrolylmethane (146 mg, 1.0 mmol) in $CHCl_3$ (200 mL) was added TFA (1.2 mg, 1 mol %). The reaction mixture was stirred in the dark for 14 h at 25 °C and subsequently treated with DDQ (227 mg, 1.0 mmol) for additional 3 h. The mixture was washed with aqueous saturated $NaHCO_3$ (50 mL) and brine (50 mL). The organic layer was dried over $MgSO_4$, filtered and concentrated under reduced pressure. Purification by flash chromatography on silica gel (CH_2Cl_2/MeOH: 98/2) gave **2** (359 mg, 50%) as a purple oil. ^{1}H NMR (300 MHz, $CDCl_3$) δ (ppm): -3.15 (s, 2H), 3.22 (s, 18H), 3.34-4.07 (m, 60H), 4.32-4.36 (m, 12H), 7.53 (s, 4H), 9.14 (d, 4H, *J* = 4.6 Hz), 9.39 (d, 4H, *J* = 4.6 Hz), 10.29 (s, 2H). These values are consistent with those reported in the literature.[23]

***5,15-Bisbromo-10,20-bis[3,4,5-tris(9-methoxy-1,4,7-trioxanonyl)phenyl]porphyrin* (3):** To a cooled (-40 °C) solution of **2** (718 mg, 0.5 mmol) in $CHCl_3$ (50 mL) was added NBS (178 mg, 1.0 mmol). After 1 h at this temperature, the reaction mixture was quenched by addition of acetone (5 mL) and the solvent was concentrated under reduced pressure. Purification by flash chromatography on silica gel (CH_2Cl_2/MeOH: 98/2) gave **3** (781 mg, 98%) as a brown oil. ^{1}H NMR (300 MHz, $CDCl_3$) δ (ppm): -2.76 (s, 2H), 3.24 (s, 18H), 3.37-4.05 (m, 60H), 4.29-4.51 (m, 12H), 7.42 (s, 4H), 8.90 (d, 4H, *J* = 4.8 Hz), 9.61 (d, 4H, *J* = 4.8 Hz).

***5,15-Bis[(4-aminophenyl)ethynyl]-10,20-bis[3,4,5-tris(9-methoxy-1,4,7-trioxanonyl)phenyl]porphyrin* (4):** To a degassed solution of **3** (1.59 g, 1.0 mmol) and 4-ethynylaniline (293 mg, 2.5 mmol) in THF (12 mL) and Et_3N (8 mL) were added $Pd_2(dba)_3$ (92 mg, 10 mol %) and $AsPh_3$ (153 mg, 0.5 mmol). The reaction mixture was stirred for 24 h at 50 °C and subsequently poured into brine (20 mL). The organic layer was dried over $MgSO_4$, filtered and concentrated under reduced pressure. Purification by flash chromatography on silica gel (CH_2Cl_2/MeOH: 97/3) gave **4** (1.50 g, 90%) as a brown oil. ^{1}H NMR (300 MHz, $CDCl_3$) δ (ppm): -1.85 (s, 2H), 3.22 (s, 18H), 3.35-4.05 (m, 60H), 4.32-4.51 (m, 12H), 6.86 (d, 4H, *J* = 8.3 Hz), 7.45 (s, 4H), 7.84 (d, 4H, *J* = 8.3 Hz), 8.84 (d, 4H, *J* = 4.7 Hz), 9.63 (d, 4H, *J* = 4.7 Hz). HRMS (ESI): calcd for $C_{90}H_{119}N_6O_{24}$ $[M+2H]^{3+}$ 555.9420, found 555.9423.

***1-(2,4-Dinitrophenyl)-1'-methyl-4,4'-bipyridinium* ($\mathbf{5}^{2+}$):** To a solution of 4,4′-bipyridine (1.56 g, 10 mmol) in acetone (50 mL) was added 1-chloro-2,4-dinitrobenzene (2.02 g, 10 mmol). The reaction mixture was stirred for 12 h at 50 °C and cooled to room temperature. The precipitate was collected by filtration, washed with Et_2O, and dried under vacuum. The crude solid was then dissolved in MeCN (100 mL) and MeOH (1 mL), before addition of MeI (2.84 g, 20 mmol). The reaction mixture was stirred for 12 h at 25 °C. The precipitate was collected by filtration, washed with Et_2O, and dried under vacuum to afford **5**ClI (3.70 g, 74%) as an orange solid. ^{1}H NMR (300 MHz, DMSO-d_6) δ (ppm): 4.48 (s, 3H), 8.45 (d, 1H, *J* = 8.7 Hz), 8.89 (d, 2H, *J* = 6.9 Hz), 9.02 (dd, 1H, *J* = 2.5 and 8.7 Hz), 9.08 (d, 2H, *J* = 7.1 Hz), 9.17 (d, 1H, *J* = 2.5 Hz), 9.36 (d, 2H, *J* = 6.9 Hz), 9.71 (d, 2H, *J* = 7.1 Hz). These values are consistent with those reported in the literature.[24]

***5,15-Bis[(4-(1-phenyl-1'-methyl-4,4'-bipyridinium))ethynyl]-10,20-bis[3,4,5-tris(9-methoxy-1,4,7-trioxanonyl)phenyl]porphyrin* ($\mathbf{6}^{4+}$):** To a solution of **5**ClI (1.50 g, 3.0 mmol) in EtOH (40 mL) and CH_3CN (20 mL) was added **4** (1.65 g, 1.0 mmol). The reaction mixture was stirred for 18 h at 70 °C and cooled to room temperature. The mixture was concentrated under reduced pressure. Purification by flash chromatography on silica gel (CH_3CN/H_2O/sat. aq. KNO_3: 6/2/2) and anion exchange using an aqueous saturated KPF_6 solution, gave **6**$(PF_6)_4$ (1.48 g, 58%) as a green solid. ^{1}H NMR (400 MHz, DMSO-d_6) δ (ppm): -2.06 (s, 2H), 3.10-4.42 (m, 90H), 4.49 (s, 6H), 7.62 (s, 4H), 8.28 (d, 4H, *J* = 8.4 Hz), 8.63

(d, 4H, *J* = 8.4 Hz), 8.93 (d, 4H, *J* = 6.4 Hz), 9.03 (d, 4H, *J* = 6.5 Hz), 9.08 (d, 4H, *J* = 4.4 Hz), 9.35 (d, 4H, *J* = 6.4 Hz), 9.83 (d, 4H, *J* = 6.5 Hz), 9.92 (d, 4H, *J* = 4.4 Hz). HRMS (ESI): calcd for $C_{112}H_{134}N_8O_{24}$ $[M]^{4+}$ 493.7372, found 493.7376.

5,15-Bis[(4-(1-phenyl-1'-methyl-4,4'-bipyridinium))ethynyl]-10,20-bis[3,4,5-tris(9-methoxy-1,4,7-trioxanonyl)phenyl]porphyrinatozinc(II) **(7^{4+}):** To a solution of **6**$(PF_6)_4$ (128 mg, 0.05 mmol) in CH_3CN (20 mL) was added $Zn(OAc)_2$ (92 mg, 0.5 mmol). The reaction mixture was stirred in the dark for 16 h at 25 °C. The mixture was concentrated under reduced pressure and an aqueous saturated KPF_6 solution (20 mL) was added. The precipitate was collected by filtration and dried under vacuum to afford **7**$(PF_6)_4$ (130 mg, 99%) as a green solid. ^{1}H NMR (400 MHz, DMSO-d_6) δ (ppm): 3.15-4.42 (m, 90H), 4.49 (s, 6H), 7.52 (s, 4H), 8.25 (d, 4H, *J* = 8.4 Hz), 8.57 (d, 4H, *J* = 8.4 Hz), 8.93 (d, 4H, *J* = 6.3 Hz), 9.02 (m, 8H), 9.35 (d, 4H, *J* = 6.3 Hz), 9.83 (m, 8H). HRMS (ESI): calcd for $C_{112}H_{132}N_8O_{24}Zn$ $[M]^{4+}$ 509.2156, found 509.2145.

Acknowledgements

The authors wish to thank the "École Doctorale de Chimie de Lyon" (PhD funding SC), the "École Normale Supérieure de Lyon" (PhD funding PH) and the GDR CNRS 2067 "Macrocycles Pyrroliques". Financial support from the TGIR-RMN-THC FR3050 is also gratefully acknowledged.

Supporting information

Additional information, NMR, HRMS, UV-visible absorption spectra, voltammetric curves are given in the supplementary material. This material is available free of charge *via* the Internet at https://www.worldscientific.com/doi/suppl/xxx.

REFERENCES

1. Schuster GB, Cafferty BJ, Karunakaran SC and Hud NV. J. Am. Chem. Soc. 2021; 143: 9279-9296.
2. Hirschi S, Ward TR, Meier WP, Müller DJ and Fotiadis D. Chem. Rev. 2022; 122: 16294-16328.
3. Forrest SR. Organic Electronics: Foundations to Applications; Oxford University Press: Oxford, 2020
4. Kahlfuss C, Saint-Aman E and Bucher C. In Organic Redox Systems: Synthesis, Properties, and Applications, Nishinaga T. (Ed.) John Wiley & Sons: Hoboken, 2016; pp 39-88.
5. Bonanno NM, Poddutoori PK, Sato K, Sugisaki K, Takui T, Lough AJ and Lemaire MT. Chem. Eur. J. 2018; 24: 14906-14910.
6. Zhan T-G, Zhou T-Y, Lin F, Zhang L, Zhou C, Qi Q-Y, Li Z-T and Zhao X. Org. Chem. Front. 2016; 3: 1635-1645.
7. Chowdhury S, Nassar Y, Guy L, Frath D, Chevallier F, Dumont E, Ramos AP, Demets GJ-F and Bucher C. Electrochim. Acta 2019; 316: 79-92.
8. Tian J, Ding Y-D, Zhou T-Y, Zhang K-D, Zhao X, Wang H, Zhang D-W, Liu Y and Li Z-T. Chem. - Eur. J. 2014; 20: 575-584.
9. Morisue M, Morita T and Kuroda Y. Org. Biomol. Chem. 2010; 8: 3457-3463.
10. Pasternack RF, Huber PR, Boyd P, Engasser G, Francesconi L, Gibbs E, Fasella P, Cerio Venturo G and Hinds Ld. J. Am. Chem. Soc. 1972; 94: 4511-4517.
11. Procházková K, Zelinger Z, Lang K and Kubát P. J. Phys. Org. Chem. 2004; 17: 890-897.
12. Dixon DW and Steullet V. J. Inorg. Biochem. 1998; 69: 25-32.
13. Kano K, Takei M and Hashimoto S. J. Phys. Chem. 1990; 94: 2181-2187.
14. Kano K, Minamizono H, Kitae T and Negi S. J. Phys. Chem. A 1997; 101: 6118-6124.
15. Kano K, Fukuda K, Wakami H, Nishiyabu R and Pasternack RF. J. Am. Chem. Soc. 2000; 122: 7494-7502.
16. Kubát P, Lang K, Procházková K and Anzenbacher P, Jr. Langmuir 2003; 19: 422-428.
17. Jeon WS, Kim H-J, Lee C and Kim K. Chem. Commun. (Cambridge, U. K.) 2002: 1828-1829.
18. Dias Correia H, Chowdhury S, Ramos AP, Guy L, Demets GJ-F and Bucher C. Polym. Int. 2019; 68: 572-588.
19. Kim H-J, Jeon WS, Ko YH and Kim K. Proc. Natl. Acad. Sci. U.S.A. 2002; 99: 5007-5011.
20. Mayhew SG. Eur. J. Biochem. 1978; 85: 535-547.

21. Dancil K-PS, Hilario LF, Khoury RG, Mai KU, Nguyen CK, Weddle KS and Shachter AM. J. Heterocycl. Chem. 1997; 34: 749-755.
22. Nielsen CB, Johnsen M, Arnbjerg J, Pittelkow M, McIlroy SP, Ogilby PR and Jørgensen M. J. Org. Chem. 2005; 70: 7065-7079.
23. Sakurai T, Shi K, Sato H, Tashiro K, Osuka A, Saeki A, Seki S, Tagawa S, Sasaki S, Masunaga H, Osaka K, Takata M and Aida T. J. Am. Chem. Soc. 2008; 130: 13812-13813.
24. Constantin V-A, Cao L, Sadaf S and Walder L. Phys. Status Solidi B 2012; 249: 2395-2398.

Redox-responsive 1D-assembly built from cucurbit[8]uril and a water-soluble metalloporphyrin-based tecton

Shagor Chowdhury, Paul Hennequin, Olivier Cala, Sandrine Denis-Quanquin, Éric Saint-Aman, Denis Frath, Floris Chevallier* and Christophe Bucher*

A linear porphyrin-based tecton bearing two viologen and two monomethyl-ether triethylene glycol-substituted phenyl units at the meso positions was synthesized and characterized. The latter was involved in the redox-triggered formation of linear supramolecular assemblies with cucurbit[8]uril cavitands in aqueous media by intermolecular π-dimerization of the viologen cation radicals after reduction.